CHARACTERIZATION OF OUT-OF-PLANE IMPACT DAMAGE IN STITCHED CFRP LAMINATES

Akinori Yoshimura*, Tomoaki Nakao, Shigeki Yashiro*** and Nobuo Takeda******
Japan Aerospace Exploration Agency, **Sumitomo Corporation,
****Ehime University, *****The University of Tokyo**

Keywords: *Stitched laminate, CFRP, Delamination, Damage extension simulation*

Abstract

The present study experimentally and numerically investigated the damage progress in stitched and unstitched CFRP laminates under the low-velocity out-of-plane impact load. First, we performed drop-weight impact tests for both stitched and unstitched specimens, and inspected the damage by using the soft X-ray radiographs and micro-focus X-ray CT. We then conducted damage-extension simulation using a layer-wise finite element model with stitch threads as beam elements, in which the damage (ply cracks and delamination) was represented by cohesive elements. A detailed comparison between the experimental and simulated results confirmed that stitching effectively suppressed the out-of-plane impact damage. Furthermore, we demonstrated that the improvement effect of impact damage resistance became greater when the impact energy was larger.

1 Introduction

Stitched CFRP laminate is a kind of three dimensional reinforced composites. In the stitched laminates, stitch threads are directed along through-the-thickness direction [1]. The stitch threads survive after the onset of delamination, and the threads bridge the delamination crack. Therefore, nominal values of interlaminar fracture toughness of stitched laminates, which are measured by DCB (Double Cantilever Beam) and ENF (End Notched Flexure) tests, are much higher than those of unstitched laminates [1-11].

Generally, conventional (unstitched) FRP laminates have low interlaminar toughness, and out-of-plane impact easily generates delamination, which significantly degrades material properties: tensile strength, compressive strength, fatigue life, etc. Among them, compressive strength is seriously reduced by delamination. Residual compressive strength after impact load (CAI strength: Compression After Impact strength) often becomes less than half of the compressive strength of intact laminate. Therefore, it is quite important to suppress the out-of-plane impact damage when the FRP laminates are used as the structural components which may receive impact load.

Because of their high interlaminar fracture toughness, it has been expected that stitched laminates have high impact damage resistance. Numerous studies conducted out-of-plane impact tests for the stitched laminates. Most of the results of these tests confirmed that the impact damage was degraded in the stitched laminates [6, 10, 12-16]. However, the intensities of the degradations were varied, moreover, some results showed that the stitching had no effect on the impact resistance of the laminates [5]. Therefore, the further discussions about the mechanism and characteristic of the degradation of impact damage due to stitching are needed.

The present study both experimentally and numerically investigates the damage process in the stitched laminates under the low velocity impact loading. In particular, we focused on the characteristic of the impact damage degradation due to stitching. The present paper is organized as follows. In Section 2, the drop-weight impact tests and detailed damage observations by using NDI technique are conducted for both stitched and unstitched laminates. In Section 3, we perform damage extension simulations of stitched laminates under the out-of-plane indentation load, and discuss the characteristics of the impact damage degradation due to stitching.

2 Experiment

2.1 Experimental Procedure

In this research, carbon-fiber stitched CFRP laminates (Toyota Industries Corp.) were used. T800-12kf tows (Toray Industries Inc.) were used as the in-plane tows, and TR-40-2kf yarns (Mitsubishi Rayon Co., Ltd.) were used as the stitch threads. Stacking sequence of the in-plane tows was $[-45/0/45/90]_{3s}$. Figure 1 illustrates the stitching pattern. Stitch threads ran along the 0° direction of the in-plane tows, and perpendicularly to the selvage yarns [17]. The stitch space and the stitch pitch were both 3.0 mm. For comparison, unstitched preform was also prepared. The fabrication procedure of the unstitched preform was the same as that of the stitched preform without the stitching process. The materials were impregnated and molded by the Resin Transfer Molding (RTM) method. For the matrix, epoxy resin system (Araldite5052 / Aradur5052) was employed. Materials were cut by diamond saw to rectangular specimens. The dimensions of specimen were 102 mm in length and 76 mm in width, where length direction was parallel to the 0° direction of the in-plane tows. The thicknesses of the specimens were about 4.5 mm.

Drop-weigtht impact test device (Instron/Dynatup 9250HV) was employed for impact tests. Figure 2 shows the impact test fixture. The picture frame type holder plate held specimen. The window shape was rectangle; size was 80 mm x 60 mm. The weight of the impactor was 5.07 kg, and the tip shape of the impactor was hemisphere of 12.7 mm in diameter. Three levels of impact energy were applied to each type of specimen: 0.8375, 1.675, 3.350 J/mm. The impact energy was normalized by the plate thickness.

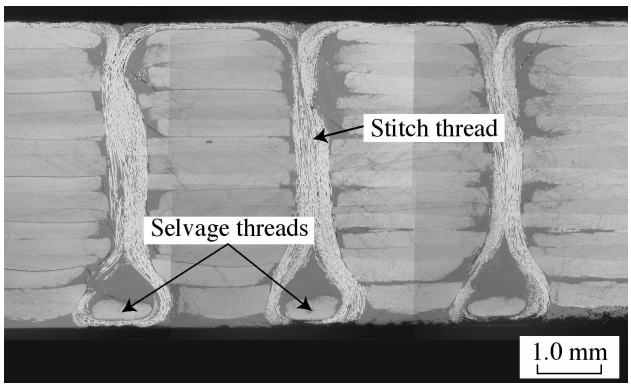

Fig. 1. Cross section of the laminate along a stitch thread.

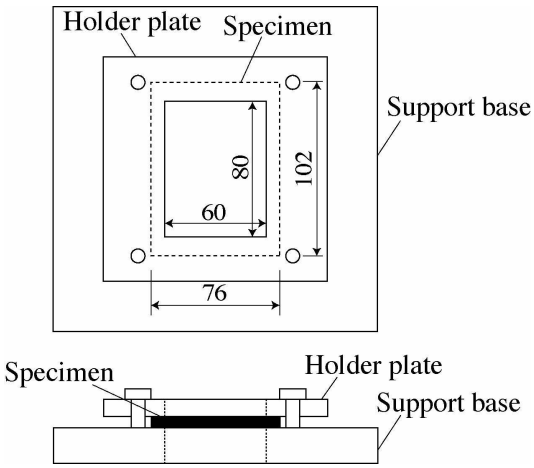

Fig. 2. Schematic of impact test fixture.

Two kinds of soft X-ray NDI were conducted for detailed observation of the impact damage. For clearly observation, contrast medium (zinc iodide) was penetrated to the specimen before inspection. For all specimens, we took soft X-ray radiographs by using general purpose soft X-ray film device (M-100S, SOFTEX, Inc.) in order to observe the in-plane distribution of the damage. For the specimens of 1.675 J/mm impact, we took section images by using soft X-ray micro-focus Computed Tomography (CT) system (TOSCANER-30000μhd, TOSHIBA IT & Control Systems Corp.) in order to observe through-the-thickness distribution of the damage.

2.2 Experimental Results

Figure 3 presents soft X-ray radiographs of the specimens. At all impact energy levels, in the unstitched specimen, one long and straight ply crack occurred in the -45° ply which located in the bottom of the specimen. The impact damage spread along the -45°crack. On the other hand, although ply cracks occurred in the stitched specimens, the cracks did not extend as long as those in the unstitched specimens. The impact damage expanded relatively equally to all direction. At all energy levels, the damage areas in the stitched laminates were smaller than those in unstitched laminates.

Figure 4 plots the projected damage area as a function of the impact energy, where the areas were obtained by processing the X-ray radiograph images. When impact energy was small, the difference of damage areas between the stitched and unstitched specimens was small. The difference became larger with increasing the impact energy, namely, the improvement effect of impact damage resistance due

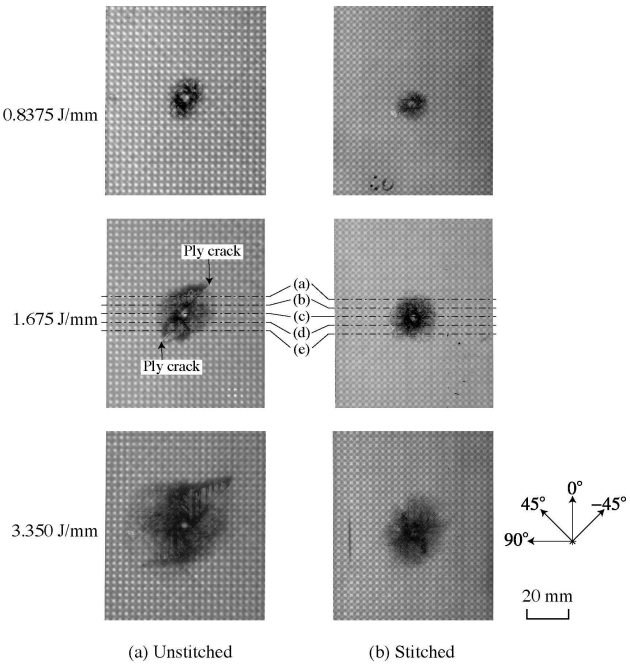

Fig. 3. Soft X-ray radiographs of the impacted specimens.

to the stitching became greater when the impact energy was larger.

Figures 5 and 6 present soft X-ray CT images of unstitched and stitched specimens, where white lines indicate cracks. The sections were indicated in Fig. 3(a)-(e). In both stitched and unstitched specimens, ply cracks and delaminations occurred, but the damage distributions in through-the-thickness direction were different between stitched and unstitched specimens. In the unstitched specimen, the damage area was small aruond the top surface, but largest around the bottom surface. In the stitched specimen, on the other hand, the damage area was small near

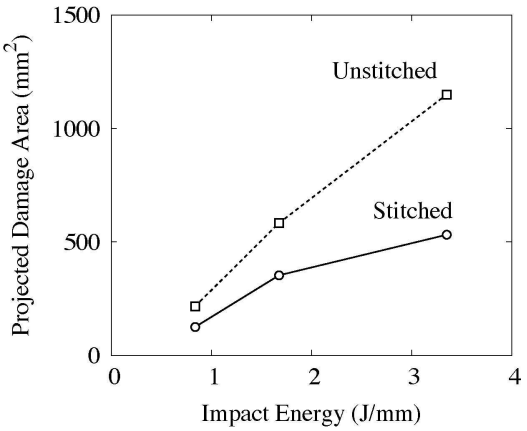

Fig. 4. Projected area of measured impact damage as a function of impact energy.

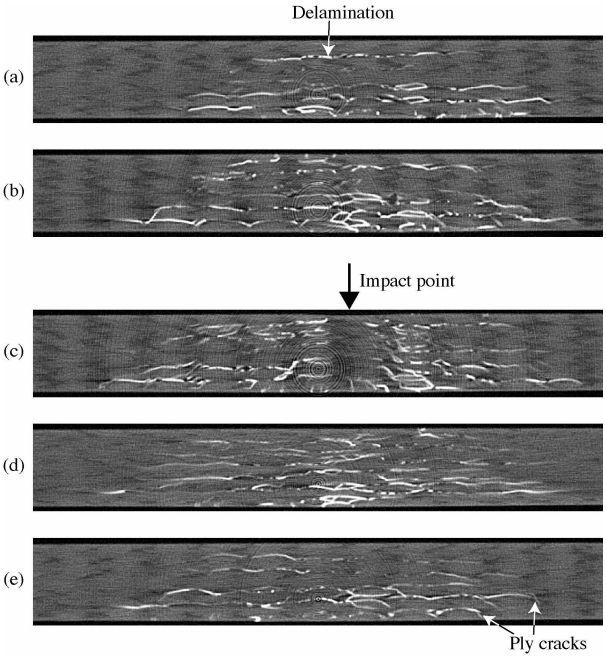

Fig. 5. Soft X-ray CT images of the unstitched specimen. White area denotes the crack penetrated by contrast medium (zinc iodide).

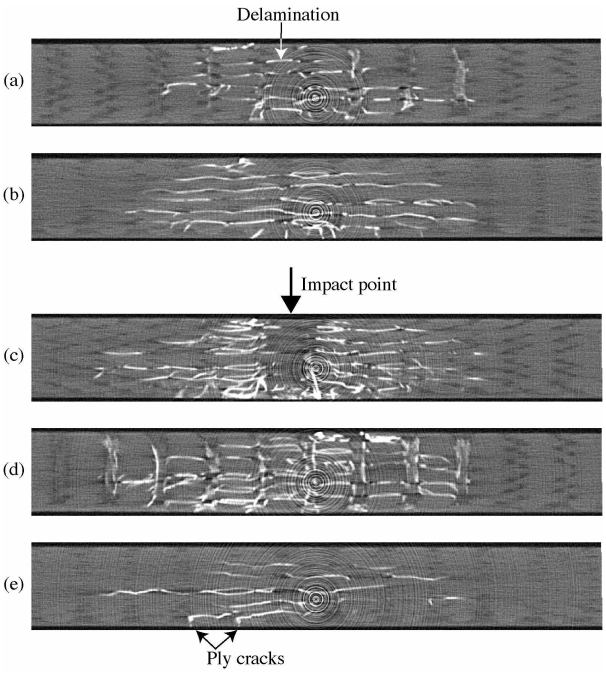

Fig. 6. Soft X-ray CT images of the stitched specimen.

the top and bottom surfaces, but largest around the center of the specimen.

3 Numerical Analysis

3.1 Analytical Model

We performed the damage extension simulations and investigated the damage process of the stitched and unstitched laminates. The velocity of the impacter used in this study was about 1.0-3.0 m/s. Thus the impact events were regarded as low velocity impact events [18]. Generally, the low velocity impact load and the static indentation load cause almost similar damage in the CFRP laminates [19]. Therefore, in the present simulation, the static indentation boundary condition was applied to the layer-wise finite element model, which was proposed by the authors [20, 21].

Figure 7(a) depicts the layer-wise finite element model that expressed the stitched laminate. The dimensions of model were 80 mm in length, 60 mm in width. The stacking sequence was $[-45/0/45/90]_{2s}$. The laminate was divided into sixteen layers, and each layer expressed the ply of each fiber direction. Each layer was divided by the four-node isoparametric Mindlin plate elements. The stitch threads were expressed by connecting the neighboring layers by two-node Timoshenko beam elements, and the beam section was circular. The beam elements were located every 3.0 mm in both x and y direction.

To express the ply cracks, four-node cohesive elements were introduced in each layer as indicated in Fig. 7(b). In addition, eight-node cohesive elements were introduced at each interface of the layers to connect the layers and to express the delamination.

For cohesive elements in the present model, we employed the bilinear relation between traction and separation that was proposed by Geubelle [22]. The present model was nonlinear due to the cohesive elements. We solved the problem by using the direct recurrent method [23], which consists of the repetition of linear analyses.

The static indentation displacement d was applied in the node located at the center of the top surface of the model, and damage extension was calculated. Note that we introduced the initial delamination of diameter of 8.0 mm in each interface in order to avoid numerical instability.

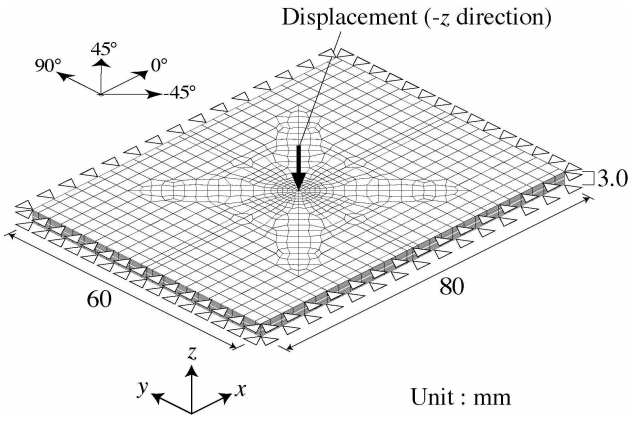

(a) Overview of the mesh

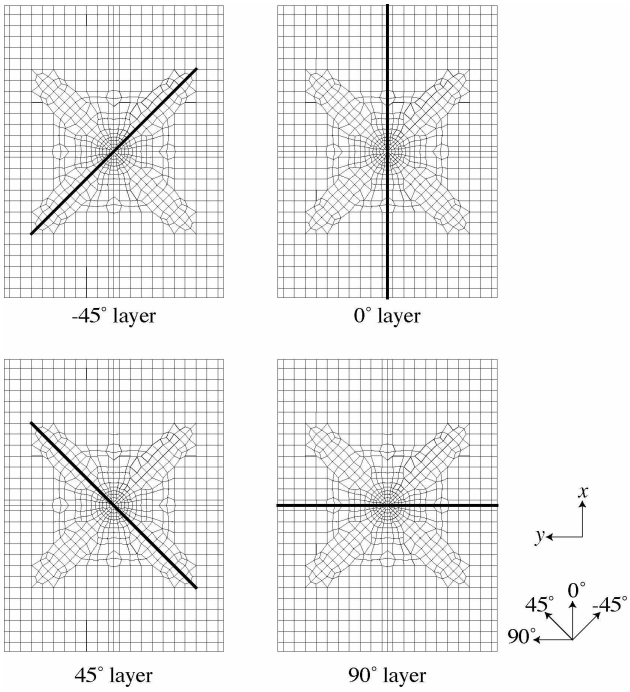

(b) Arrangement of the cohesive elements in the each layer.

Fig. 7. Layer-wise finite element model for the damage extension simulation under the out-of-plane indentation load.

3.2 Simulation Results

Table 1 and 2 present the material properties and the parameters of cohesive elements used in the present analysis. For the critical energy release rates for ply cracks, the catalogue values of the epoxy resin system were used. For the critical energy release rates of delamination, we employed the typical

Table 1. Material properties of a stitched laminate.

(a) Laminate	
Longitudinal Young's modulus E_x (GPa)	120.83
Transverse Young's modulus $E_y = E_z$ (GPa)	9.57
Longitudinal shear modulus $G_{xy} = G_{xz}$ (GPa)	4.50
Transeverse shear modulus G_{yz} (GPa)	3.50
Longitudinal Poisson's ratio $\nu_{xy} = \nu_{xz}$	0.356
Transeverse Poisson's ratio ν_{yz}	0.49
(b) Stitch thread	
Longitudinal Young's modulus E_z (GPa)	148.0
Longitudinal shear modulus $G_{xz} = G_{yz}$ (GPa)	4.5
Diameter (mm)	0.6

Table 2. Parameters of the cohesive elements used in the simulation.

(a) Ply crack	
In-plane tensile strength (Mode I, MPa)	40.0
In-plane shear strength (Mode II, MPa)	60.0
Out-of-plane shear strength (Mode III, MPa)	60.0
Critical energy release rate (Mode I, J/m^2)	100.0
Critical energy release rate (Mode II, J/m^2)	500.0
Critical energy release rate (Mode III, J/m^2)	500.0
(b) Delamination	
In-plane tensile strength (Mode I, MPa)	40.0
In-plane shear strength (Mode II, MPa)	60.0
Out-of-plane shear strength (Mode III, MPa)	60.0
Critical energy release rate (Mode I, J/m^2)	200.0
Critical energy release rate (Mode II, J/m^2)	1000.0
Critical energy release rate (Mode III, J/m^2)	1000.0

values of interlaminar toughness of CFRP from literatures.

Figure 8 plots the distribution of delamination when the indentation displacement d was about 3.0 mm. In the figure, the points denote the cohesive elements which fractured completely, and the color of the points indicates the interface. In addition, black bold lines denote the ply cracks of the -45° layers. In this figure, the indentation displacement was applied at the point $(x, y, z) = (0.0, 0.0, 3.0)$.

In the unstitched model, delamination which located closer to the bottom of the model extended larger(Fig. 8(a)), and similarly, the ply cracks which located closer to the bottom extended larger. The longest ply crack occurred at the bottom of the model because of the flexure deformation of the model. At the neighboring -45°/0° interface, delamination expanded along the -45° layer crack because of the peel deformation of the model. Therefore, the

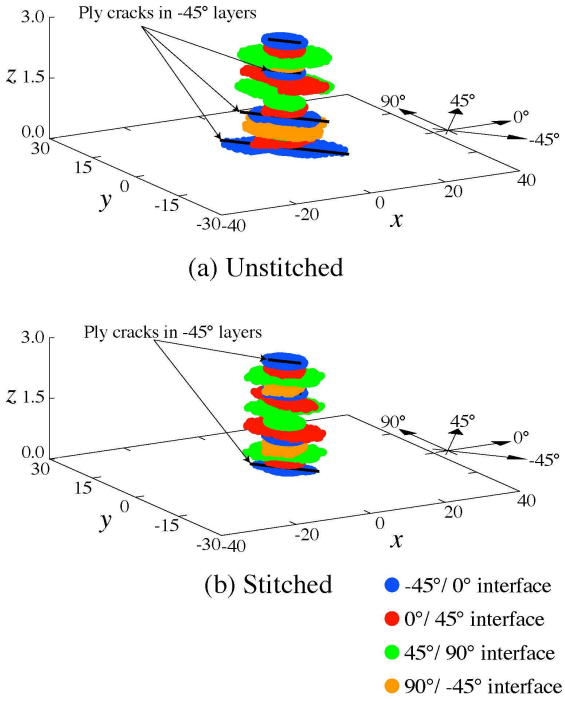

Fig. 8. Simulation results for three dimensional distribution of delamination under out-of-plane indentation load (d = 3.0 mm). Bold black lines indicate ply cracks in -45° layers.

xy projected shape of the delamination was large in the -45° direction.

On the other hand, in the stitched model (Fig. 8(b)), although the longest ply crack occurred at the bottom of the model, the delamination of the neighboring -45°/0° interface did not extend particularly larger than those of the other interfaces. The areas of delaminations which located near the center in the thickness direction were slightly larger than the other delaminations, but the difference was not so large. Moreover, in the stitched model, the delamination expanded relatively equally to all direction. The reason of these phenomena was that the stitch threads suppressed the peel deformation of the model, and delamination did not extend large near the bottom of the model.

Figure 9 plots the delamination area projected to xy plane as a function of the work applied to the model. Delamination area of the stitched model was always smaller than that of the unstitched model. Moreover, as the applied work became larger, the increasing rate of the delamination area became larger in the unstitched model, whereas became smaller in the stitched model. Therefore, when the impact energy was larger, the difference of the delamination area between the stitched and unstitched model grew

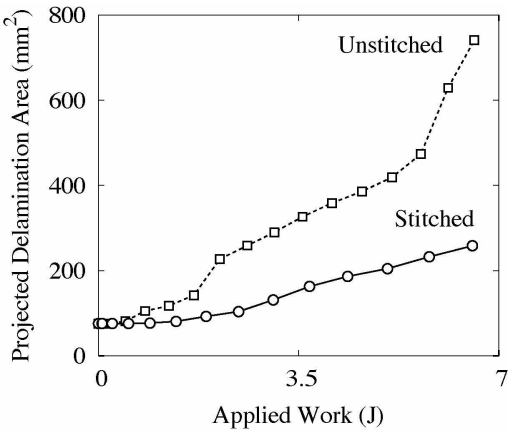

Fig. 9. Projected delamination area as a function of the energy applied to the model.

larger, namely, improvement effect of the damage resistance became greater. The impact loading with the larger energy caused increasing number of stitch threads that bridged the delamination, following the onset of the larger delamination. We concluded that these threads yielded the increase of the crack closure force, which relaxed the stress concentration at the delamination tip and finally suppressed the extension of the delamination.

4 Conclusion

The present study both experimentally and numerically investigates the damage process in the stitched laminates under the low velocity impact loading.

1. Both experimental and numerical results demonstrated that the out-of-plane impact resistance of CFRP laminates was improved by stitching.
2. In the thickness direction, the largest damage occurred around the bottom of the specimen in the unstitched laminate. On the other hand, in the stitched laminate, the largest damage occurred around the center of the specimen. The simulation results revealed that the reason of this difference was the suppression of the peel deformation due to the stitching.
3. The improvement effect of the damage resistance became greater when the impact energy was larger. We concluded that the larger impact energy caused increasing number of stitch threads that bridged the delamination, and the increasing of crack closure force achieved more effective improvement of damage resistance of the laminate.

Acknowledgement

A. Yoshimura is supported by the Ministry of Education, Culture, Sports, Science and Technology of Japan under a Grant-in-Aid for Scientific Research (No. 16-11471).

References

[1] Tong L., Mouritz A. P. and Bannister M. K. "*3D Fiber Reinforced Polymer Composites,*" Elsevier Science Ltd., 2002.

[2] Dransfield K., Baillie C. and Mai Y. M., "Improving the delamination resistance of CFRP by stitching - a review," *Compos. Sci. Technol.* Vol. 50, No. 3, pp 305–317, 1994.

[3] Jain L. and Mai Y. W., "On the effect of stitching on mode I delamination toughness of laminated composites," *Compos. Sci. Technol.* Vol. 51, No. 3, pp. 331–345, 1994.

[4] Jain L. and Mai Y. W., "Determination of mode II delamination toughness of stitched laminated composites," *Compos. Sci. Technol.* Vol. 55, No. 3, pp. 241–253, 1995.

[5] Mouritz A. P., Gallagher J. and Goodwin A. A., "Flexural strength and interlaminar shear strength of stitched GFP laminates following repeated impacts," *Compos. Sci. Technol.* Vol. 57, No. 5, pp. 509–522, 1997.

[6] Larsson F., "Damage tolerance of a stitched carbon/epoxy laminate," *Composites Part A*, Vol. 28A, No. 11, pp. 923–934, 1997.

[7] Dransfield K. A., Jain L. K. and Mai Y. W., "On the effects of stitching in CFRPs - I. Mode I delamination toughness," *Compos. Sci. Technol.* Vol. 58, No. 6, pp. 815–827, 1998.

[8] Jain L. K., Dransfield K. A. and Mai Y. W., "On the effects of stitching in CFRPs -II. Mode II delamination toughness," *Compos. Sci. Technol.* Vol. 58, No. 6, pp. 829–837, 1998.

[9] Iwahori Y., Ishikawa T., Hayashi Y. and Watanabe N., "Study of interlaminar fracture toughness improvement on stitched CFRP laminates," *J. Japan Soc. Compos. Mater.*, Vol. 26, No. 3, pp. 90–100, 2000.

[10] Mouritz A. P., "Ballistic impact and explosive blast resistance of stitched composites," *Composites Part B*, Vol. 32B, No. 5, pp. 431–439, 2001.

[11] Iwahori Y., Sugimoto S., Hayashi Y., Hori S., Ishikawa T., and Fukuda H., "Study of mechanical properties under through-the-thickness loads for stitched CFRP laminates by using tension test specimens with a single stitch thread," *J. Japan Soc. Compos. Mater.*, Vol. 32, No. 1, pp. 22-31, 2006.

[12] Liu D., "Delamination resistance in stitched and unstitched composite plates subjected to impact loading," *J. Reinf. Plast. Compos.*, Vol. 9, No. 1, pp. 59–69, 1990.

[13] Wu E. and Liau J., "Impact of unstitched and stitched laminates by line loading," *J. Compos. Mater.*, Vol. 28, No. 17, pp. 1640–1658, 1994.

[14] Wu E. and Wang J., "Bahavior of stitched laminates under in-plane tensile and transverse impact loading," *J. Compos. Mater.*, Vol. 29, No. 17, pp. 2254–2279, 1995.

[15] Hosur M. V., Adya M., Alexander J., Jeelani S., Vaidya U. and Mayer A., "Studies on impact damage resistance of affordable stitched woven/epoxy composite laminates," *J. Reinf. Plast. Compos.*, Vol. 22, No. 10, pp. 927–952, 2003.

[16] Herszberg I. and Weller T., "Impact damage resistance of buckled carbon/epoxy panels," *Compos. Struct.*, Vol. 73, No. 2, pp. 130–137, 2006.

[17] Kamiya R., Cheeseman B. A., Popper P. and Wei C. T., "Some recent advantages in the fabrication and design of three-dimensional textile preforms: a review," *Compos. Sci. Technol.*, Vol. 60, No. 1, pp. 33–47, 2000.

[18] Richardson M. O. W. and Wisheart M. J., "Review of low-velocity impact properties of composite materials," *Composite Part A*, Vol. 27A, No. 12, pp. 1123–1131, 1996.

[19] Nettles A. T. and Douglas M. J., "A comparison of quasi-static indentation to lowvelocity impact," NASA TP-2000-210481, 2000.

[20] Yashiro S., Takeda N., Okabe T. and Sekine H., "A new approach to predicting multiple damage states in composite laminates with embedded FBG sensors," *Compos. Sci. Technol.* Vol. 65, No. 3-4, pp. 659–667, 2005.

[21] Yoshimura A., Yashiro S., Okabe T. and Takeda N., "Characterization of tensile damage progress in stitched CFRP laminates," *Adv. Compos. Mater.* in–press., 2007

[22] Geubelle P. H. and Baylor J. S., "Impact-induced delamination of composites: a 2D simulation," *Composites Part B*, Vol. 29B, No. 5, pp. 589–602, 1998.

[23] Owen D. R. J. "*Finite Elements in Plasticity*," Pineridge Press, 1980.